Redshift-space distortions from vector perturbations. II. Anisotropic signal

Vittorio Tansella,[1] Camille Bonvin,[1] Giulia Cusin,[2] Ruth Durrer,[1] Martin Kunz,[1] and Ignacy Sawicki[3]

[1] *Départment de Physique Théorique and Center for Astroparticle Physics, Université de Genève, Quai E. Ansermet 24, CH-1211 Genève 4, Switzerland*

[2] *Astrophysics Department, University of Oxford, DWB, Keble Road, Oxford OX1 3RH, United Kingdom*

[3] *CEICO, Institute of Physics of the CAS, Na Slovance 2, 182 21 Praha 8, Czech Republic*

(Received 27 August 2018; published 14 November 2018)

We study the impact on the galaxy correlation function of the presence of a vector component in the tracers' peculiar velocities, in the case in which statistical isotropy is violated. We present a general framework—based on the bipolar spherical harmonics expansion—to study this effect in a model independent way, without any hypothesis on the origin or the properties of these vector modes. We construct six new observables, that can be directly measured in galaxy catalogs in addition to the standard monopole, quadrupole, and hexadecapole, and we show that they completely describe any deviations from isotropy. We then perform a Fisher analysis in order to quantify the constraining power of future galaxy surveys. For an example, we show that the SKA2 would be able to detect anisotropic rotational velocities with amplitudes as low as 1% of that of the vorticity generated during shell crossing in standard dark matter scenarios.

DOI: 10.1103/PhysRevD.98.103515

I. INTRODUCTION

Vector perturbations are generated during the history of the Universe by many mechanisms extending standard cosmology, e.g. topological defects [1–3], magnetic fields [4], inflation with vector fields [5,6], or vector-field-based models of modified gravity [7–10]. But, even in concordance cosmology, the inevitable shell crossing that occurs as non-linear structures form, leads to the generation of vorticity and therefore vector perturbations. It is important to properly characterize the signature of these vector degrees of freedom (d.o.f.) on the observables of large-scale galaxy surveys. The reason for this is twofold. On the one hand, the presence of such vector perturbations—if not properly taken into account—will "pollute" (i.e., bias) the measurement of the scalar d.o.f. and act as a source of systematic error. On the other hand, vector d.o.f. can leave their imprint on observables, which, in turn, can be used to constrain their properties and to study the mechanism that generated them.

Various approaches exist in the literature with the aim of constraining vector-type deviations of the metric, and they have mostly focused on the cosmic microwave background (CMB). They can be grouped into three categories:

(i) The first category is introducing dynamical vector d.o.f. in the early Universe while maintaining isotropy and homogeneity at the background level. Then, one can either maintain statistical isotropy and homogeneity of the perturbations or allow for statistically anisotropic perturbations [11,12].

(ii) Alternatively, one can deform the isotropy of the cosmological background and therefore constrain its anisotropy, while keeping the matter content standard, making sure that this anisotropy decays with time [13].

(iii) Finally, one can introduce an anisotropy directly in the primordial power spectrum (through some interactions in the early Universe, e.g., Refs. [14,15]). One then tries to look for "anomalies" in the CMB, such as in, e.g., Ref. [16]. Signatures of this primordial signal in galaxy surveys have been analyzed in Refs. [17–20].

Additionally, late time nonlinear evolution, as it is simulated in N-body codes, is found to generate vector perturbations of both the metric [21,22] and the fluid vorticity [23,24]. Vorticity is generated in N-body simulations by shell crossing. The velocity and especially its vorticity are difficult to measure precisely in an N-body code. The usual techniques measure a coarse grained velocity field which exhibits additional vorticity due to coarse graining. Recently, in Ref. [25], a novel technique was developed to measure the mean velocity field averages over phase space, which is independent of any coarse graining size. It is interesting to develop statistical tools to measure these vector modes, which are present also in standard ΛCDM cosmology, and to distinguish them, e.g., from an intrinsic, global anisotropy.

In Ref. [26], some of us considered the impact of statistically isotropic vector modes in the peculiar velocity field of galaxies and in particular on the redshift-space distortion (RSD) observed in galaxy surveys. We have found that vector contributions to RSD enter in the monopole, quadrupole, and hexadecapole of the galaxy correlation function. While the impact of vector perturbations from topological defects is very small, those from nonlinear clustering affect especially the hexadecapole quite strongly, contributing up to 20% of the total signal on scales smaller than 5 h^{-1} Mpc. This additional contribution should in principle be detectable with next generation surveys, such as Euclid or the Square Kilometre Array (SKA).

In this paper, we consider a vector component of the peculiar velocities, which violates statistical isotropy, and study its impact on the galaxy correlation function. This is a natural generalization of the study in Ref. [26]. We present a general framework suitable specifically to study this effect, with no assumptions on the origin or properties of these vector modes. We show that the anisotropic signal can be completely characterized by six new observables, which can be directly extracted from galaxy catalogs. General results regarding the Fisher analysis of these types of models are also discussed. We investigate the detectability of these contributions, for a specific example, with planned or futuristic galaxy surveys.

This paper can be considered as a contribution to testing the cosmological principle. In particular, we want to develop tests of statistical isotropy using large-scale structure (LSS) observations. While it is clear that our Universe is not strongly anisotropic, a small anisotropy is still compatible with, if not favored by, the analysis of CMB anisotropies and polarization [16]. This might be due to, e.g., a small global magnetic field or some slight anisotropy which remained after inflation. In this work, we do not make assumptions on the model responsible for the global anisotropy in the vector sector, but we want to investigate its observational consequences. We study the situation where scalar perturbations are still statistically isotropic but vector perturbations are not. It will be interesting not only to study whether LSS also favors a slight anisotropy of the Universe but whether the characteristics of any such anisotropy are in agreement with the one of the CMB. Furthermore, LSS observations allow for a tomographic approach; i.e., we can observe many different redshifts, making it easier to overcome limitations from cosmic variance.

The paper is structured as follows. In Sec. II, we detail the general anisotropic structure of vector perturbations. In Sec. III, we study the effects of a vector component in the velocity field on the two-point function and present a suitable decomposition to describe it. Finally, in Sec. IV, we forecast the constraints on the anisotropic parameters for upcoming clustering surveys.

II. VECTOR CONTRIBUTION TO GALAXY VELOCITIES

In this work, we assume that our Universe shows signs of a violation of statistical isotropy, manifesting itself by the presence of vector modes in the peculiar velocity of tracers. We investigate how galaxy catalogs can be used, independently from other probes, to constrain the amplitude of these anisotropies. We therefore model our Universe as a perturbed Friedman-Lemaître universe, with a metric given by

$$\mathrm{d}s^2 = a^2[-(1+2\Psi)\mathrm{d}\tau^2 - \Sigma_i \mathrm{d}\tau \mathrm{d}x^i + (1-2\Phi)\mathrm{d}x_i \mathrm{d}x^i]. \tag{1}$$

Here, Φ and Ψ are the standard Newtonian-gauge scalar potentials, and Σ_i is a pure vector fluctuation, $\partial_i \Sigma^i = 0$, related to frame dragging.[1] We define $\mathcal{H} = \dot{a}/a = aH$ to be the conformal Hubble parameter.

The general velocity field for galaxies located at position $\boldsymbol{r}$ at conformal time τ, $v^i(\boldsymbol{r},\tau)$, can be decomposed into a scalar (potential) part, v, and a pure vector part, Ω^i, with $\partial_i \Omega^i = 0$,

$$v^i \equiv \partial^i v + \Omega^i. \tag{2}$$

The gauge-invariant relativistic vorticity [27] can be obtained by lowering the index of Ω^i with the perturbed metric. The relativistic vorticity is often denoted Ω_i (e.g., in Refs. [27,28]), and it is an additional rotational velocity over and above the frame-dragging effect. In this paper, we denote it by $\tilde{\Omega}_i \equiv g_{ij}\Omega^j/a = a\delta_{ij}(\Omega^j - \Sigma^j)$ for clarity.[2] We mainly concentrate on Ω^i as it is the velocity with an upper index that is relevant for us, and we use the notation $\Omega_i = \delta_{ij}\Omega^j \equiv \Omega^i$.

We assume that galaxies move on timelike geodesics of the metric, i.e., they obey the Euler equation. Then, to first order in perturbation theory, we can write, for perfect fluids,

$$\dot{\Omega}_i - \dot{\Sigma}_i + \mathcal{H}(\Omega_i - \Sigma_i) = 0, \tag{3}$$

which is equivalent to $\partial_\tau \tilde{\Omega}_i = 0$. Hence, vorticity is conserved. This is not only true within linear perturbation theory but also in full General Relativity as long as matter can be described as a perfect fluid [28]. The $0i$ component of the energy momentum tensor of a perfect fluid is given by

$$T^i_{0(V)} = [(\rho + P)v^i]_{(V)} = T^i_0 - T^i_{0(S)}. \tag{4}$$

Taking the curl of this equation, the scalar part vanishes, and we obtain

[1] We have fixed the gauge such that the $0i$ component of the metric has no scalar contribution and the vector part of the ij component vanishes. We also neglect gravitational waves (tensor perturbations).

[2] The difference between $a\Omega^j$ and $\tilde{\Omega}_j$ is only relevant on large scales.

$$\epsilon_{ijk}(T^j_0)_{,k} = \epsilon_{ijk}[(\rho+P)v^j]_{,k} = (\boldsymbol{v}\wedge\boldsymbol{\nabla}(\rho+P))_i + (\rho+P)(\boldsymbol{\nabla}\wedge\boldsymbol{v})_i. \quad (5)$$

Only the vector velocity Ω^j contributes to the second term, while the first term is nonvanishing when the gradient of the density fluctuations is not parallel to the velocity. This also happens in perfect fluids at second order in perturbation theory; see, e.g., Ref. [22]. At second order therefore, despite vorticity conservation, vector perturbations of the metric are generated. They, in turn, induce effects such as frame dragging. It has been shown recently [24] that the vector potential found in relativistic numerical simulations is actually mainly due to the first term of (5) and not to vorticity, which is also induced in N-body simulations.

The perfect fluid description is just an approximation when we want to describe the motion of dark matter (or galaxies). In the real Universe, dark matter particles are free streaming; i.e., they move on geodesics. As soon as shell crossing occurs, velocity dispersion can no longer be neglected, and vorticity is generated for the fluid of the averaged dark matter particles (or galaxies). In Ref. [29], the vorticity generation from large-scale structure was modeled by including velocity dispersion using a perturbative approach.

Clearly, even if in the standard ΛCDM model vector perturbations are generated by nonlinearities, they are statistically isotropic. In this work, we assume that the vectorial part of the peculiar velocity in Eq. (2) acquires an anisotropic component.

A. Tensor structure of vector perturbations

We summarize here the discussion we presented in Sec. 2.2 of Ref. [26].

In order to compute the two-point correlation function of galaxies, we need a model for the two-point autocorrelation of the vector velocity, $\langle\Omega_i\Omega_j\rangle$, and its cross-correlation with the dark matter overdensity $\langle\delta_{\rm m}\Omega_i\rangle$. We will characterize their structure in Fourier space, with our Fourier transform convention fixed by

$$f(\boldsymbol{k}) = \int d^3r f(\boldsymbol{r})e^{-i\boldsymbol{k}.\boldsymbol{r}}. \quad (6)$$

The autocorrelation of the vector field takes the general form

$$\langle\Omega_i(\boldsymbol{k})\Omega_j(\boldsymbol{k}')\rangle = (2\pi)^3\delta^{(3)}(\boldsymbol{k}+\boldsymbol{k}') \times [W_{ij}(\mathbf{k})P_\Omega(k) + i\alpha_{ij}(\mathbf{k})P_A(k)], \quad (7)$$

where $P_\Omega(k)$ and $P_A(k)$ contain information about the amplitude of the vector field. The Dirac delta function appearing in the above equation, $\delta^{(3)}(\boldsymbol{k}+\boldsymbol{k}')$, is a consequence of statistical homogeneity, and if we assume that scalar spectra are isotropic, the amplitudes, $P_\Omega(k)$ and $P_A(k)$, depend on $\mathbf{k}$ only through its absolute value $k\equiv|\mathbf{k}|$. One might think it would be more natural for an anisotropic spectrum to show an anisotropy also in $P_\Omega(\boldsymbol{k})$. However, in a real observation, the power spectrum is usually obtained by averaging the squared Fourier modes over directions. Here, we mimic this by considering P_Ω and P_A to be functions of the modulus k only. In practice, these are the direction averaged spectra. For scalar perturbations, this averaging removes all signs of an anisotropy, and for vector perturbations this is, interestingly, not the case as we show in this paper.

The tensors W_{ij} and α_{ij} are, respectively, symmetric and antisymmetric tensors, which encode the dependence on direction. Since Ω_i is a pure vector field, W_{ij} and α_{ij} must satisfy $k^iW_{ij} = k^jW_{ij} = k^i\alpha_{ij} = k^j\alpha_{ij} = 0$. The P_A-term is parity odd, while the P_Ω-term is parity even. If no parity violating processes occur in the Universe, we may set $P_A = 0$. The tensorial form for α_{ij} is completely fixed by antisymmetry and transversality,

$$\alpha_{ij} = \alpha\varepsilon_{ijm}\hat{k}^m. \quad (8)$$

The most general form for W_{ij} is then

$$W_{ij} = \frac{\omega}{2}(\delta_{ij} - \hat{k}_i\hat{k}_j) + \omega^A_{ij}, \quad (9)$$

where we have decomposed the tensor into its trace ω and trace-free part

$$\omega^A_{ij} = \omega_{ij} - \omega_{il}\hat{k}^l\hat{k}_j - \omega_{lj}\hat{k}^l\hat{k}_i + \omega_{lm}\hat{k}^l\hat{k}^m\hat{k}_i\hat{k}_j, \quad (10)$$

with $\omega^i_i = 0$. As usual, $\hat{\boldsymbol{k}}$ denotes the unit vector in the direction of the vector $\boldsymbol{k}$. The first term of (9) respects statistical homogeneity and isotropy, whereas the second one is nonzero only when isotropy is violated. In what follows, we absorb the trace ω into the normalization of the power spectrum P_Ω in Eq. (7). Note that in general the isotropic and anisotropic contribution do not need to have the same amplitude $P_\Omega(k)$; in this sense, one can use $\omega(k)$ to parametrize the difference between $P^{(\rm iso)}_\Omega$ and $P^{(\rm ani)}_\Omega$. Interestingly, the only possible parity odd term given in (8) is statistically isotropic.

The symmetric tensor ω_{ij} can be diagonalized or, equivalently, decomposed into a sum of the tensor products of its orthonormal eigenvectors $\hat{\omega}^I_i$,

$$\omega_{ij} = \sum_{I=1}^{3}\lambda_I\hat{\omega}^I_i\hat{\omega}^I_j, \quad (11)$$

where the eigenvalues satisfy $\sum_I\lambda^I = 0$.

The cross-correlation with dark matter can be nonzero only if statistical isotropy is violated. Assuming that the vector field is fluctuating in some fixed direction $\hat{\boldsymbol{\omega}}$, the cross-correlation takes the form

$$\langle \delta_{\rm m}(\boldsymbol{k})\Omega_i(\boldsymbol{k}')\rangle = (2\pi)^3 W_i P_{\delta\Omega}(k)\delta^{(3)}(\boldsymbol{k}+\boldsymbol{k}'), \quad (12)$$

where W_i is transverse since Ω_i is a pure vector field, i.e., divergence free. A nonvanishing $\langle \delta_{\rm m}\Omega_i\rangle$ always defines a preferred spatial direction $\hat{\omega}_i$ and therefore violates statistical isotropy.

III. CORRELATION FUNCTION

Galaxy number counts are observed in redshift space, rather than in real space. The leading correction arising from the fact that we observe on the light cone is the Kaiser term, or redshift-space distortion [30], which is included in the number counts Δ as

$$\Delta(\boldsymbol{r}) = \delta_{\rm g}(\boldsymbol{r}) - \frac{1}{\mathcal{H}} n^i\partial_i(n^j v_j(\boldsymbol{r})). \quad (13)$$

Here, δ_g is the tracer's density perturbation, related to the dark matter density perturbation via the bias expansion $\delta_g \simeq b\cdot\delta_m + \ldots$, and v_i is the peculiar velocity field. We have also defined the line-of-sight direction $\boldsymbol{n}$ as

$$\boldsymbol{n} \equiv \frac{\boldsymbol{r}}{r}, \quad (14)$$

i.e., the unit vector in the direction of the galaxy lying at $\boldsymbol{r}$, with the observer located at $\boldsymbol{r}=0$. Splitting the velocity into the scalar and vector parts, as in Eq. (2), we have

$$\Delta(\boldsymbol{r}) = \delta_{\rm g}(\boldsymbol{r}) - \frac{1}{\mathcal{H}} n^i n^j(\partial_i\partial_j v(\boldsymbol{r}) + \partial_i\Omega_j(\boldsymbol{r})). \quad (15)$$

The effects of vector perturbations in the general relativistic number counts were derived in Ref. [31] and studied in detail in Ref. [32], where it was found that—akin to scalar perturbations—redshift-space distortion is the dominant effect. Since in the relativistic angular power spectra, $C_\ell(z_1,z_2)$, the RSD cannot easily be extracted, we study here the impact of the vector modes on the two-point correlation function of galaxies. In this study, we neglect both the subdominant vector relativistic corrections from Ref. [32] and the scalar relativistic corrections derived in Refs. [33–37].

The two-point correlation function is defined as

$$\xi(\boldsymbol{r}_1,\boldsymbol{r}_2,z_1,z_2) = \langle\Delta(\boldsymbol{r}_1,z_1)\Delta(\boldsymbol{r}_2,z_2)\rangle. \quad (16)$$

Without redshift-space distortion, and neglecting subdominant evolution effects, the correlation function depends only on the galaxies' separation

$$x \equiv |\boldsymbol{r}_1 - \boldsymbol{r}_2| \quad (17)$$

and on the mean distance of the pair from the observer $\bar{r} = \frac{1}{2}(r_1+r_2)$ or, equivalently, its mean redshift $\bar{z} = \frac{1}{2}(z_1+z_2)$. Redshift-space distortion introduces an additional dependence on the orientation of the pair with respect to the line of sight $\mathbf{n}$ (we work in the small angle or flat-sky limit where we neglect the difference between the line of sight to $\boldsymbol{r}_1$ and $\boldsymbol{r}_2$). It is customary to expand ξ in a basis of Legendre polynomials so that, in the flat-sky approximation, $\boldsymbol{n}_1=\boldsymbol{n}_2=\boldsymbol{n}$, we can write

$$\xi(\bar{z},\mathbf{x},\mathbf{n}) = \sum_\ell \xi_\ell(\bar{z},x)\mathcal{P}_\ell(\mu), \quad (18)$$

where $\mathcal{P}_\ell$ is the Legendre polynomial of degree ℓ and $\mu = \boldsymbol{n}\cdot\hat{\boldsymbol{x}}$, with $\hat{\boldsymbol{x}}$ being the direction of the vector connecting the two galaxies.

Let us now review the standard flat-sky expression for the correlation function in the presence of scalar perturbations (see, e.g., Ref. [38] for details). We will use this result both for comparison with the vector case and to compute our covariance matrix in Sec. IV. Including the Kaiser term, we write

$$\xi^{\rm iso}_{\rm (s)}(\bar{z},x,\mu) = c_0(\bar{z})C_0(\bar{z},x) - c_2(\bar{z})C_2(\bar{z},x)\mathcal{P}_2(\mu) + c_4(\bar{z})C_4(\bar{z},x)\mathcal{P}_4(\mu). \quad (19)$$

We can identify the multipole coefficients in Eq. (18) as

$$\xi_\ell(x,\bar{z}) = i^\ell c_\ell(\bar{z})C_\ell(\bar{z},x). \quad (20)$$

We have also defined

$$C_\ell(\bar{z},x) = \int \frac{{\rm d}k}{2\pi^2}k^2 P(\bar{z},k)j_\ell(kx), \quad (21)$$

together with the coefficients

$$c_0 = b^2 + \frac{2}{3}bf + \frac{f^2}{5}, \quad (22)$$

$$c_2 = \frac{4}{3}bf + \frac{4}{7}f^2, \quad (23)$$

$$c_4 = \frac{8}{35}f^2. \quad (24)$$

Here, j_n is the n-order spherical Bessel function, f is the growth rate, $f \equiv d\ln D_1/d\ln a$ (with D_1 being the linear growth function), and $P(\bar{z},k)$ is the matter power spectrum at redshift $\bar{z}$. We have made the standard assumption that the galaxy bias b is deterministic, and, like the growth rate f in ΛCDM, it is scale independent.

We now turn to the study of the vector component. We split the vector contribution to the correlation function into a statistically isotropic and anisotropic part

$$\xi_{(\mathrm{v})} = \xi_{(\mathrm{v})}^{\mathrm{iso}} + \xi_{(\mathrm{v})}^{\mathrm{ani}}, \tag{25}$$

where we have emphasized that the source of violation of statical isotropy comes from the vector sector. First, we summarize the structure of the isotropic contributions to the correlation function coming from vector perturbations, and we then propose a general framework to compute the anisotropic part.

The new vector contribution to the correlation function in Eq. (25) comprises three terms:

(1) cross-correlation with the density
(2) cross-correlation with the scalar velocity
(3) autocorrelation.

The first two vanish in flat sky since they are odd under $\boldsymbol{n} \to -\boldsymbol{n}$ and ξ is evidently even; see Ref. [26]. Hence, combining Eqs. (15) and (16), we write

$$\xi_{(\mathrm{v})}(x) = \frac{1}{\mathcal{H}(z_1)\mathcal{H}(z_2)} \int \frac{\mathrm{d}^3 k}{(2\pi)^3} k^2 (\boldsymbol{n}_1 \cdot \hat{\boldsymbol{k}})(\boldsymbol{n}_2 \cdot \hat{\boldsymbol{k}}) \times n_1^i W_{ij}(\hat{\boldsymbol{k}}) n_2^j P_\Omega(k) e^{i\boldsymbol{k}\cdot\boldsymbol{x}}. \tag{26}$$

This object has a complicated tensor structure, which characterizes the anisotropy of the vector field. However, when isotropy is assumed, we simply write $W_{ij} = \delta_{ij} - \hat{k}_i \hat{k}_j$, so that, see Ref. [26],

$$\xi_{(\mathrm{v})}^{\mathrm{iso}} = \frac{1}{\mathcal{H}^2} \int \frac{\mathrm{d}^3 k}{(2\pi)^3} k^2 (\boldsymbol{n} \cdot \hat{\boldsymbol{k}})^2 (1 + (\boldsymbol{n} \cdot \hat{\boldsymbol{k}})^2) \times P_\Omega(k) e^{i\boldsymbol{k}\cdot\boldsymbol{x}}. \tag{27}$$

Rewriting the $\boldsymbol{n} \cdot \hat{\boldsymbol{k}}$ contributions in terms of Legendre polynomials and integrating over the direction of $\boldsymbol{k}$, we obtain for the isotropic contribution [26]

$$\xi_{(\mathrm{v})}^{\mathrm{iso}}(\bar{z}, x, \mu) = \frac{2}{15} \mathcal{P}_0(\mu) C_0^\Omega(x) - \frac{2}{21} \mathcal{P}_2(\mu) C_2^\Omega(x) - \frac{8}{35} \mathcal{P}_4(\mu) C_4^\Omega(x), \tag{28}$$

with

$$C_n^\Omega(x) = \frac{1}{2\pi^2} \frac{1}{\mathcal{H}^2} \int \mathrm{d}k k^4 P_\Omega(k) j_n(kx). \tag{29}$$

Notice here the extra k^2 factor multiplying P_Ω, which is absorbed in the scalar case when the velocity power spectrum is reexpressed in terms of the density power spectrum.

Statistically isotropic vector perturbations modify the shape of the multipoles coefficients in the Legendre expansion of ξ. One can estimate this effect and study its detectability. This was the strategy followed in Ref. [26]. In the anisotropic case, however, the standard multipole expansion fails to capture the additional angular dependence encoded in W_{ij}. In the next section, we therefore consider the decomposition of this dependence into bipolar spherical harmonics (BipoSH) [39].

A. Statistically anisotropic contribution

When statistical isotropy is violated, the correlation function is no longer only a function of $\mu = \boldsymbol{n} \cdot \hat{x}$. Therefore, the standard expansion in Legendre polynomials does not properly describe the angular dependence of ξ. The correlation function can, however, be expanded in terms of the orthonormal set of BipoSH. Since this approach captures an arbitrary angular dependence of the observable under consideration, it has been used in cosmology to analyze CMB [40–45] and LSS [15,19,20,46–51] data.

In the small angle approximation the correlation function depends on two directions $\xi(\mathbf{n}, \mathbf{x})$, and we hence expand

$$\xi(\mathbf{x}, \mathbf{n}, \bar{z}) = \sum_{\ell\ell' JM} \xi_{\ell\ell'}^{JM}(x, \bar{z}) X_{\ell\ell'}^{JM}(\hat{\mathbf{x}}, \mathbf{n}), \tag{30}$$

with

$$X_{\ell\ell'}^{JM}(\hat{\mathbf{x}}, \mathbf{n}) = \{Y_\ell(\hat{\mathbf{x}}) \otimes Y_{\ell'}(\mathbf{n})\}_{JM} = \sum_{mm'} \mathbf{C}_{\ell m \ell' m'}^{JM} Y_{\ell m}(\hat{\mathbf{x}}) Y_{\ell' m'}(\mathbf{n}), \tag{31}$$

where $\mathbf{C}_{\ell m \ell' m'}^{JM}$ are the Clebsch-Gordan coefficients which are related to the Wigner 3j symbols by, see Ref. [52],

$$\mathbf{C}_{\ell m \ell' m'}^{JM} = (-)^{\ell - \ell' + M} \sqrt{2J+1} \begin{pmatrix} \ell & \ell' & J \\ m & m' & -M \end{pmatrix}. \tag{32}$$

In other words, $X_{\ell\ell'}^{JM}(\hat{\mathbf{x}}, \mathbf{n})$ isolates the total angular momentum J and helicity M contribution. The useful property of the BipoSH $X_{\ell\ell'}^{JM}$ is that they filter the isotropic signal into the $J=0$ mode and any nonzero coefficient with $J>0$ indicates anisotropy. In fact, if there is no anisotropic signal in the power spectrum, i.e., if ξ depends on $\mathbf{n}$ only via $\mu = \hat{\mathbf{x}} \cdot \mathbf{n}$, we can compute the coefficients via

$$\xi_{\ell\ell'}^{JM} = \int d\Omega_{\mathbf{n}} \int d\Omega_{\mathbf{x}} \xi(\mathbf{x}, \mathbf{n}, \bar{z}) X_{\ell\ell'}^{JM*}, \tag{33}$$

and we simply obtain

$$\xi_{\ell\ell'}^{JM}(x, \bar{z}) = \frac{4\pi}{\sqrt{2\ell+1}} \xi_\ell(x, \bar{z}) \delta_{J,0} \delta_{M,0} \delta_{\ell,\ell'}, \tag{34}$$

recovering the expansion of Eq. (18). In particular, we see that no off-diagonal component is generated (we have $\ell = \ell'$) and that all the isotropic signal is contained in the $J=0$ coefficient. On the other hand, if anisotropy is included, we will generate $J \geq 1$ and $\ell \neq \ell'$ modes.

Therefore, to search for anisotropy, we only look at the $J \geq 1$ modes, and we set $\xi = \xi^{\mathrm{ani}}_{(\mathrm{v})}$ in the expansion of Eq. (30).

We focus on the computation of the statistically anisotropic contribution to the galaxy correlation function (16). To this end, it is useful to compute the anisotropic contribution to the power spectrum of (13) and then Fourier transform it. Explicitly, the Fourier transformation of galaxy number counts in the Kaiser approximation, Eq. (13), is given by

$$\langle \tilde{\Delta}(\mathbf{k}, \mathbf{n}, \bar{z}) \tilde{\Delta}(\mathbf{k}', \mathbf{n}, \bar{z}) \rangle = (2\pi)^3 P(\mathbf{k}, \mathbf{n}, \bar{z}) \delta(\mathbf{k} + \mathbf{k}'), \quad (35)$$

where the power spectrum is given by (omitting the dependence on $\mathbf{n}, \bar{z}$)

$$\begin{aligned} P(\mathbf{k}) &= P^{\mathrm{iso}}_{(\mathrm{s})} + P^{\mathrm{iso}}_{(\mathrm{v})} + P^{\mathrm{ani}}_{(\mathrm{v})} \\ &= (b + f(\mathbf{n} \cdot \hat{\mathbf{k}})^2)^2 P_{\delta\delta}(k) \\ &\quad - \frac{k^2}{\mathcal{H}^2} \omega (\mathbf{n} \cdot \hat{\mathbf{k}})^2 (1 - (\mathbf{n} \cdot \hat{\mathbf{k}})^2) P_{\Omega}(k) \\ &\quad - \frac{k^2}{\mathcal{H}^2} (\mathbf{n} \cdot \hat{\mathbf{k}})^2 \hat{n}^i n^j \omega^A_{ij} P_{\Omega}(k), \end{aligned} \quad (36)$$

where all the isotropic contribution is in the first two lines and the anisotropic one, $P^{\mathrm{ani}}_{(\mathrm{v})}$, is in the last line. The tensor ω^A_{ij} is defined in Eq. (10). The isotropic contribution depends on directions only through the angle between the mode $\mathbf{k}$ and the line of sight; i.e., it can be expanded in a basis of Legendre polynomials as

$$P^{\mathrm{iso}}(\mathbf{k}, \mathbf{n}, \bar{z}) = \sum_{\ell} p_{\ell}(k, \bar{z}) \mathcal{P}_{\ell}(\mathbf{n} \cdot \hat{\mathbf{k}}). \quad (37)$$

We observe that this is not a specific property of redshift-space distortions but simply a consequence of statistical isotropy. Hence, Eq. (37) holds for all the relativistic contributions to the galaxy number counts.

When statistical isotropy is violated, we expand the power spectrum in terms of the orthonormal set of bipolar spherical harmonics, as

$$P^{\mathrm{ani}}_{(\mathrm{v})}(\mathbf{k}, \mathbf{n}, \bar{z}) = \sum_{\ell\ell' JM} \pi^{JM}_{\ell\ell'}(\bar{z}, k) X^{JM}_{\ell\ell'}(\hat{\mathbf{k}}, \mathbf{n}), \quad (38)$$

where

$$X^{JM}_{\ell\ell'}(\hat{\mathbf{k}}, \mathbf{n}) = \sum_{mm'} \mathbf{C}^{JM}_{\ell m \ell' m'} Y_{\ell m}(\hat{\mathbf{k}}) Y_{\ell' m'}(\mathbf{n}). \quad (39)$$

In the case where there is not anisotropic signal in the power spectrum, the coefficients $\pi^{JM}_{\ell\ell'}$ simply reduce to

$$\pi^{JM}_{\ell\ell'} = \frac{4\pi}{\sqrt{2\ell + 1}} p_{\ell}(k) \delta_{J,0} \delta_{M,0} \delta_{\ell,\ell'}, \quad (40)$$

and we recover the expansion of Eq. (37).

For convenience, we can split the anisotropic contribution to the power spectrum (36) in three contributions

$$\begin{aligned} P^{\mathrm{ani}}_{(\mathrm{v})}(\mathbf{k}) &= - \frac{k^2}{\mathcal{H}^2} (\mathbf{n} \cdot \hat{\mathbf{k}})^2 \hat{n}^i \hat{n}^j \omega^A_{ij} P_{\Omega}(k) \\ &= P^{(\mathrm{a})}(\mathbf{k}) + P^{(\mathrm{b})}(\mathbf{k}) + P^{(\mathrm{c})}(\mathbf{k}), \end{aligned} \quad (41)$$

where we have separated the three cases

(a) $\omega^A_{ij} = \omega_{ij}$,

(b) $\omega^A_{ij} = -\omega_{il} \hat{k}^l \hat{k}_j - \omega_{lj} \hat{k}^l \hat{k}_i$,

(c) $\omega^A_{ij} = \omega_{lm} \hat{k}^l \hat{k}^m \hat{k}_i \hat{k}_j$,

so that

$$\begin{aligned} &P^{\mathrm{ani}}_{(\mathrm{v})}(\mathbf{k}, \mathbf{n}, \bar{z}) \\ &\quad = \sum_{\ell\ell' JM} (\pi^{JM(\mathrm{a})}_{\ell\ell'} + \pi^{JM(\mathrm{b})}_{\ell\ell'} + \pi^{JM(\mathrm{c})}_{\ell\ell'}) X^{JM}_{\ell\ell'}(\hat{\mathbf{k}}, \mathbf{n}). \end{aligned} \quad (42)$$

Note that this splitting has no direct physical interpretation; each contribution has a scalar component, which, however, disappears in the sum of Eq. (42). These contributions can be written in terms of the eigenvectors and eigenvalues $\hat{\omega}^I$ and λ_I. After a long but straightforward computation, we find

$$\begin{aligned} \pi^{JM(\mathrm{a})}_{\ell\ell'} &= - \frac{16\pi^{3/2}}{45} \frac{k^2}{\mathcal{H}^2} P_{\Omega}(k) \sum_I \lambda_I Y^*_{2M}(\hat{\omega}_I) \\ &\quad \times \left(\delta_{\ell,0} \delta_{\ell',2} + 2 \sqrt{\frac{2\ell' + 1}{5}} \begin{pmatrix} 2 & 2 & \ell' \\ 0 & 0 & 0 \end{pmatrix} \delta_{\ell,2} \right) \delta_{J,2}, \end{aligned} \quad (43)$$

$$\begin{aligned} \pi^{JM(\mathrm{b})}_{\ell\ell'} = &- \frac{16\pi^{3/2}}{5} \frac{k^2}{\mathcal{H}^2} P_{\Omega}(k) \sqrt{(2\ell + 1)(2\ell' + 1)} \\ &\times \sqrt{\frac{2}{15}} \sum_I \lambda_I Y^*_{2M}(\hat{\omega}_I) \\ &\times \left[2 \begin{pmatrix} 3 & 1 & \ell \\ 0 & 0 & 0 \end{pmatrix} \begin{pmatrix} 3 & 1 & \ell' \\ 0 & 0 & 0 \end{pmatrix} \begin{Bmatrix} 1 & 2 & 1' \\ \ell & 3 & \ell' \end{Bmatrix} \right. \\ &\left. + 3 \begin{pmatrix} 1 & 1 & \ell \\ 0 & 0 & 0 \end{pmatrix} \begin{pmatrix} 1 & 1 & \ell' \\ 0 & 0 & 0 \end{pmatrix} \begin{Bmatrix} 1 & 2 & 1 \\ \ell & 1 & \ell' \end{Bmatrix} \right] \delta_{J,2}, \end{aligned} \quad (44)$$

$$\begin{aligned} \pi^{JM(\mathrm{c})}_{\ell\ell'} &= - \frac{16\pi^{3/2}}{15} \frac{k^2}{\mathcal{H}^2} P_{\Omega}(k) \sum_I \lambda_I Y^*_{2M}(\hat{\omega}_I) \\ &\quad \times \left[\frac{1}{5} \delta_{\ell,2} \delta_{\ell',0} + \frac{8}{105} \sqrt{2\ell + 1} \begin{pmatrix} 4 & 2 & \ell \\ 0 & 0 & 0 \end{pmatrix} \delta_{\ell',4} \right. \\ &\quad \left. + \frac{4}{7\sqrt{5}} \sqrt{2\ell + 1} \begin{pmatrix} 2 & 2 & \ell \\ 0 & 0 & 0 \end{pmatrix} \delta_{\ell',2} \right] \delta_{J,2}, \end{aligned} \quad (45)$$

where curly brackets {} denote the Wigner 6j symbols; see, e.g., Ref. [53]. We first note that vector anisotropies can only generate $J = 2$ modes. This is not surprising as they are the product of two $j = 1$ states which can give either $J = 0$, which is isotropic, or $J = 2$. The triangular relation imposed by the 3j and 6j symbols determines the limits of the sum in the expansion in Eq. (42). It is easy to see that both ℓ and ℓ' have to be even and, more precisely, in $\{0, 2, 4, 6\}$. We can now reconstruct the correlation function (16) from the power spectrum. This is similar to the isotropic case in which the Fourier- and real-space coefficients in the Legendre expansion are related by

$$\xi_\ell(x) = i^\ell \int \frac{k^2 dk}{2\pi^2} j_\ell(kx) p_\ell(k). \tag{46}$$

Explicitly, the coefficients of the BipoSH expansion of the correlation function, Eq. (30), are related to the ones of the power spectrum, Eq. (38), by

$$\xi^{JM}_{\ell\ell'}(x) = i^\ell \int \frac{k^2 dk}{2\pi^2} j_\ell(kx) \pi^{JM}_{\ell\ell'}(k). \tag{47}$$

With this, we can rewrite the real-space version of Eqs. (43)–(45) in terms of the C^Ω_n, which we defer to an Appendix: Eqs. (C1)–(C3). The sum of the three contributions can be cast in matrix form as (remember all terms with $J \neq 2$ vanish)

$$(\xi^{2M}_{\ell\ell'}) = \frac{16\pi^{3/2}}{5} \sum_I \lambda_I Y^*_{2M}(\hat\omega_I) \times \begin{pmatrix} 0 & 0 & \frac{1}{35}C^\Omega_0 & 0 & 0 & 0 & 0 \\ 0 & 0 & 0 & 0 & 0 & 0 & 0 \\ \frac{1}{25}C^\Omega_2 & 0 & -\frac{1}{5}\sqrt{\frac{2}{35}}C^\Omega_2 & 0 & \frac{2}{225}\sqrt{\frac{2}{7}}C^\Omega_2 & 0 & 0 \\ 0 & 0 & 0 & 0 & 0 & 0 & 0 \\ 0 & 0 & 0 & 0 & -\frac{4}{9\sqrt{385}}C^\Omega_4 & 0 & 0 \\ 0 & 0 & 0 & 0 & 0 & 0 & 0 \\ 0 & 0 & 0 & 0 & -\frac{8}{63\sqrt{55}}C^\Omega_6 & 0 & 0 \end{pmatrix}, \tag{48}$$

where $C^\Omega_\ell = C^\Omega_\ell(z, x)$. Equation (48) is one of the main results of this paper. It shows in complete generality that *any* anisotropic signal induced by redshift-space distortion in the galaxy correlation function is encoded in the functions $\xi^{2M}_{\ell\ell'}$ (which depend in principle on redshift and on galaxy separation). The six nonzero coefficients $\boldsymbol{\xi} = \{\xi^{2M}_{02}, \xi^{2M}_{20}, \xi^{2M}_{22}, \xi^{2M}_{24}, \xi^{2M}_{44}, \xi^{2M}_{64}\}$ are therefore the equivalent of the monopole, quadrupole, and hexadecapole that are measured in standard redshift surveys, when anisotropies are assumed to be absent. As we will show below, these six coefficients can be directly extracted from catalogs of galaxies, by averaging over pairs of galaxies with an appropriate weighting. A detection of a nonzero $\xi^{2M}_{\ell\ell'}$ would represent a smoking gun for the presence of anisotropies in the galaxies peculiar velocities. Note that the dependence of the $\xi^{2M}_{\ell\ell'}$ on the model responsible for the anisotropies is encoded in the $C^\Omega_\ell(z, x)$ and in the eigenvectors $\hat\omega_I$ and eigenvalues λ_I. In the following, we construct estimators for the six nonzero coefficients $\boldsymbol{\xi}$, and we forecast the detectability of these coefficients with future surveys.

IV. FORECAST FOR LSS SURVEYS

We now forecast the constraints on the anisotropy parameters—which we define later—as expected from future redshift surveys. In the next section, we define our estimators for the BipoSH coefficients and compute their covariance matrix. For simplicity, and since here we are only interested in the anisotropic signal, we fix all standard cosmological parameters to their Planck best fit values in this analysis. We expect the degeneracies with standard cosmological parameters to be very mild; nevertheless, marginalization over them would probably increase the uncertainties somewhat.

A. Estimator and covariance

To estimate the expansion coefficients, the obvious choice is to weight the correlation function by $X^{2M}_{\ell\ell'}$, in the same way that we weight the two-point function by the Legendre polynomials $\mathcal{P}_\ell$ to estimate the multipoles. In a binned survey, the estimator is

$$\hat\xi^{2M}_{\ell\ell'}(x) = a_N \sum_{i,j} \Delta_i \Delta_j X^{2M*}_{\ell\ell'}(\hat x_{ij}, \hat n_{ij}) \delta_K(x_{ij} - x), \tag{49}$$

where δ_K is the Kronecker delta, Δ_i is the galaxy overdensity in the bin labeled by the index i, and we have defined $\mathbf{x}_{ij} = \mathbf{x}_i - \mathbf{x}_j$, $\mathbf{n}_{ij} = 1/2(\mathbf{x}_i + \mathbf{x}_j)$. The normalization factor a_N is found by imposing that the estimator is unbiased,

$$\langle \hat\xi^{2M}_{\ell\ell'} \rangle = \xi^{2M}_{\ell\ell'}, \tag{50}$$

in the continuous limit

$$\sum_i \to \frac{1}{L_p^3} \int d^3x_i, \ \delta_K(x_{ij} - x) \to L_p \delta_D(x_{ij} - x), \tag{51}$$

where L_p denotes the pixel size and V is the total volume of the survey. We obtain

$$a_N = \frac{3L_p^5}{Vx^2}. \tag{52}$$

We also have $a_N = 1/N(x)$, where $N(x)$ is the number of pixels which contribute to the estimator. The variance of the estimator is defined as

$$\mathrm{var}(\hat{\xi}^{2M}_{\ell\ell'}) \equiv \mathrm{var}^M_{\ell\ell'} = \langle(\hat{\xi}^{2M}_{\ell\ell'})^2\rangle - \langle\hat{\xi}^{2M}_{\ell\ell'}\rangle^2, \tag{53}$$

and we recall that $\langle\Delta_i\Delta_j\rangle$ contains a Poisson noise contribution and a cosmic variance (CV) contribution,

$$\langle\Delta_i\Delta_j\rangle = \frac{1}{d\bar{n}}\delta_{ij} + C^{\Delta}_{ij}, \tag{54}$$

where $d\bar{n}$ is the mean number of galaxies per pixel. The correlation C^{Δ}_{ij} is due both to the scalar and vector parts of Δ. However, the scalar component strongly dominates over the vector one, so that we can neglect the latter. Physically, this reflects the fact that, even though the coefficients $\xi^{2M}_{\ell\ell'}$ are constructed to remove the scalar isotropic signal and to isolate the vector anisotropic signal, the covariance of these coefficients is still affected (and dominated) by the scalar contribution. We then obtain three different contributions to the variance which are understood respectively as the Poisson term (P), the mixed term (M), and the CV term (C). Explicitly, we find

$$\mathrm{var}_P(x,x') = \frac{6V}{x^2N^2_{\mathrm{tot}}}\delta_D(x-x'), \tag{55}$$

$$\mathrm{var}_M(x,x') = \frac{24}{\pi N_{\mathrm{tot}}}\int dkk^2P(k,\bar{z})j_\ell(kx)j_\ell(kx') \times \sum_w c_w\beta^w_{\ell\ell'}, \tag{56}$$

$$\mathrm{var}_C(x,x') = \frac{12}{\pi V}\int dkk^2P^2(k,\bar{z})j_\ell(kx)j_\ell(kx') \times \sum_\sigma \tilde{c}_\sigma\beta^\sigma_{\ell\ell'}, \tag{57}$$

where N_{tot} is the total number of tracers in the catalog and the indices w, σ take values $w = 0, 2, 4$ and $\sigma = 0, 2, 4, 6, 8$. The explicit form of the coefficients $\beta^\sigma_{\ell\ell'}$ and details on the derivation of the various contributions of the variance can be found in Appendix A, where we also compute the covariance matrix of the estimator, defined as

$$\mathrm{cov}(\hat{\xi}^{2M_1}_{\ell_1\ell_1'}, \hat{\xi}^{2M_2}_{\ell_2\ell_2'}) \equiv \mathrm{cov}^{M_1M_2}_{\ell_1\ell_1'\ell_2\ell_2'} = \langle\hat{\xi}^{2M_1}_{\ell_1\ell_1'}\hat{\xi}^{2M_2}_{\ell_2\ell_2'}\rangle - \langle\hat{\xi}^{2M_1}_{\ell_1\ell_1'}\rangle\langle\hat{\xi}^{2M_2}_{\ell_2\ell_2'}\rangle. \tag{58}$$

B. Fisher forecasts

We now want to forecast the constraints on the anisotropic parameters from a survey. Given a model for the anisotropy power spectrum, i.e., a parametrization for P_Ω, we are left with the 5 d.o.f. of the symmetric traceless tensor ω_{ij} and an overall amplitude A_V for the vector power spectrum, which can be reabsorbed in a redefinition of ω_{ij}. Following our decomposition in Eq. (11), we identify the d.o.f. as the eigenvalues and eigenvectors of ω_{ij}. On the one hand, the eigenvalues are of zero sum so that we can pick the first two λ_1, λ_2 as independent and the third one is fixed to $-(\lambda_1+\lambda_2)$. On the other hand, we find it convenient to parametrize the three orthonormal eigenvectors $\hat{\omega}_I$ in terms of the three angles of an Euler rotation which rotates the canonical basis of $\mathbb{R}^3$ into the $\hat{\omega}_I$,

$$\hat{\omega}_I \equiv R(\alpha,\beta,\gamma)\cdot\hat{e}_I, \tag{59}$$

where $\hat{e}_I$ are the three orthonormal vectors of $\mathbb{R}^3$ and $R(\alpha,\beta,\gamma)$ is the rotation matrix with Euler angles α, β, γ. Furthermore, we can absorb the amplitude A_V in the eigenvalues by defining $\tilde{\lambda}_I = A_V\lambda_I$. In summary, the 5 d.o.f. of the tensor $\bar{\omega}_{ij}$ and the overall amplitude A_V are encoded in our parameter space

$$\theta = \{\tilde{\lambda}_1, \tilde{\lambda}_2, \alpha, \beta, \gamma\}. \tag{60}$$

The Fisher matrix is defined as

$$F_{\theta\theta'} \equiv \frac{1}{2}\frac{\partial^2\chi^2}{\partial\theta\partial\theta'} = \sum_{\mathcal{A},\mathcal{A}'}\frac{\partial\langle\hat{\xi}_{\mathcal{A}}\rangle}{\partial\theta}\bigg|_{\mathrm{f}}\mathrm{cov}^{-1}_{\mathcal{A}\mathcal{A}'}\frac{\partial\langle\hat{\xi}^*_{\mathcal{A}'}\rangle}{\partial\theta'}\bigg|_{\mathrm{f}}, \tag{61}$$

where, schematically, $\mathcal{A} = \{\ell_1, \ell_1', M_1, x_i, z_1\}$, $\mathcal{A}' = \{\ell_2, \ell_2', M_2, x_j, z_2\}$, and the derivatives are evaluated at the fiducial model. The Fisher matrix contains therefore a sum over the six nonzero coefficients which constitute our data, over all pixels separations x_i, x_j and over all bins of redshifts z_i, z_j. The covariance matrix properly accounts for all correlations between these quantities, except for the correlations between different redshift bins $z_i \neq z_j$, which we assume to be uncorrelated, since the bin size that we consider is sufficiently large. We then have

$$\mathrm{cov}_{\mathcal{A}\mathcal{A}'} = \mathrm{cov}_{\ell_1\ell_1'\ell_2\ell_2'}(x_i,x_j)\delta_{M_1M_2}\delta_{z_1z_2}. \tag{62}$$

We recall that, according to the Cramer-Rao inequality, the Fisher matrix provides a lower bound on the marginal parameter uncertainty σ_θ as

$$\sigma_\theta \geq \sqrt{(F^{-1})_{\theta\theta}}. \tag{63}$$

We start by constraining the parameters λ_1, λ_2. The submatrix is then written

$$\begin{aligned} F_{\tilde{\lambda}_A\tilde{\lambda}_B} &= \sum_{\{z_{\mathrm{bin}}\}}\sum_{i,j}\sum_{\ell_1\ell_1'\ell_2\ell_2'}\sum_M \frac{\partial\xi^M_{\ell_1\ell_1'}(x_i,z)}{\partial\tilde{\lambda}_A}\mathrm{cov}^{-1}_{\ell_1\ell_1'\ell_2\ell_2'}(x_i,x_j) \times \frac{\partial\xi^{M*}_{\ell_2\ell_2'}(x_j,z)}{\partial\tilde{\lambda}_B} \\ &= \sum_{\{z_{\mathrm{bin}}\}}\sum_{i,j}\sum_{\ell_1\ell_1'\ell_2\ell_2'}\frac{5}{4\pi}(2+\mathcal{P}_2(\delta_{AB}))\tilde{\xi}_{\ell_1\ell_1'}(x_i,z) \\ &\quad\times \mathrm{cov}^{-1}_{\ell_1\ell_1'\ell_2\ell_2'}(x_i,x_j)\tilde{\xi}^*_{\ell_1\ell_1'}(x_j,z), \end{aligned} \tag{64}$$

where we have defined

$$\xi^{2M}_{\ell_1\ell'_1} \equiv A_V \sum_I \lambda_I Y^*_{2M}(\hat{\omega}_I)\tilde{\xi}_{\ell_1\ell'_1} \tag{65}$$

by explicitly writing the amplitude A_V of P_Ω out of the C^Ω_ℓ. We normalize this amplitude such that $\lambda_{\max} \equiv 1$. The variables which determine the anisotropy are then the amplitude A_V, the ratio $\lambda_2/\lambda_1 = \lambda_2$, and the three angles (α, β, γ) which determine the orientation. For the second equal sign of Eq. (64), we have performed the sum over M using that

$$\frac{\partial \xi^{2M}_{\ell_1\ell'_1}}{\partial \tilde{\lambda}_A} = Y^*_{2M}(\hat{\omega}_A)\tilde{\xi}_{\ell_1\ell'_1} - Y^*_{2M}(\hat{\omega}_3)\tilde{\xi}_{\ell_1\ell'_1}, \tag{66}$$

together with the orthogonality properties of products of spherical harmonics. We observe that the final result does not depend on the fiducial values of the parameters $\tilde{\lambda}_I$ since they enter linearly in the estimator $\hat{\xi}^{2M}_{\ell_1\ell_2}$. We also note that we did not need to fix any fiducial direction $\hat{\omega}_I$ since the dependence on $\hat{\omega}_I$ cancels out in the final result.

In Appendix B, we show that the off-diagonal blocks of the full Fisher matrix (61) are vanishing; hence, $F_{\theta\theta'}$ has a block-diagonal structure,

$$[F_{\theta\theta'}] = \left[\begin{array}{c|c} F_{\lambda_A\lambda_B} & \mathbf{0} \\ \hline \mathbf{0} & F_{\alpha\beta\gamma} \end{array}\right]. \tag{67}$$

As a consequence of the block structure of the Fisher matrix, it follows that the constraints on the amplitudes λ_I can be derived directly with Eq. (64). In particular, they do not depend on the fiducial values of the eigenvectors $\hat{\omega}_I$. This reflects the fact that the precision with which we can measure the eigenvalues does not depend on the direction of the anisotropy. The constraints on directions, i.e., $(\sigma_\alpha, \sigma_\beta, \sigma_\gamma)$, can be obtained by inverting the lower block of the Fisher matrix. It turns out that the constraints on each of the directions depend on the fiducial values of both the eigenvalues and the eigenvectors of $\bar{\omega}_{ij}$. However, this direction dependence is somewhat artificial, as we could have chosen our basis directions differently. Instead of considering each direction independently, it makes more sense to compute the volume of the ellipsoid described by the constraints on (α, β, γ), using the Haar measure $\mathrm{d}\mu = \sin\beta \mathrm{d}\alpha \mathrm{d}\beta \mathrm{d}\gamma$. Note that with this non-normalized Haar measure, the volume of the rotation group $SO(3)$ is $2(2\pi)^2 \simeq 79$. We can think of this uncertainty volume as the inverse of a "figure of merit" for the average accuracy with which we can recover the directional information. This combined direction constraint has the great advantage that it does not depend on the fiducial model for the directions but only on the choice of the eigenvalues' ratio λ_A/λ_B and the vector amplitude A_V. This remaining dependence is physical and simply reflects the fact that the precision with which we can measure the direction of the anisotropy does obviously depend on how large it is.

C. Model for vector perturbations

To illustrate how our general formalism can be used, we consider an explicit model in which a nonisotropic vector contribution to the galaxy peculiar velocities gives new contributions to the correlation function. We derive constraints on the directions and amplitudes of anisotropies for both a Euclid-like and a SKA2-like survey. The specifications for these surveys are taken from Refs. [54,55], respectively; the two redshift ranges are $z \in [0.7, 2.0]$ for Euclid and $z \in [0.1, 2.0]$ for SKA2, and we split them into 14 and 19 bins of thickness $\Delta z = 0.1$ respectively, with $L_p = 2$ Mpc$/h$. This choice of L_p is motivated by the fact that this pixel size gives the best constraints in Ref. [26]. Note that in the isotropic case exploiting separations as small as 2 Mpc$/h$ does require a good understanding of the scalar nonlinear signal at those scales, which is highly nontrivial. In the anisotropic case, however, since the scalar part does not contribute to the estimators $\hat{\xi}^{2M}_{\ell\ell'}$, but only to the covariance, we can exploit very small separations even without a very precise modeling of the scalar behavior at those scales. For maximum separation, we choose 40 Mpc$/h$.

Until this point, our formalism has been model independent, but, clearly, to forecast the detectability of the anisotropy parameters, we have to assume a shape for $P_\Omega(k)$. For an example, we choose the isotropic vorticity power spectrum from N-body simulations, while we note that, as we have stated before, the isotropic and anisotropic P_Ω can in principle be different.

According to the numerical simulations of Refs. [23,24], the vorticity power spectrum appears to evolve as $\mathcal{H}(z)^2 f(z)^2 D_1(z)^7$ at large scales. At small scales, the evolution has an additional scale dependence, leading to a suppression of power at small scales at late times; see Fig. 4 of Ref. [23]. In the following, we will ignore this small-scale dependence and assume that the power spectrum at redshift z is given by[3]

$$P_\Omega(k,z) = P_\Omega(k, z=0)\left(\frac{\mathcal{H}(z)f(z)}{\mathcal{H}_0 f(z=0)}\right)^2 \left(\frac{D_1(z)}{D_1(z=0)}\right)^7.$$

We use the vorticity power spectrum plotted in Fig. 4 of Ref. [23] to construct the following fit for P_Ω,

$$P_\Omega(k, z=0) = A_V \frac{(k/k_*)^{n_\ell}}{[1 + (k/k_*)]^{n_\ell + n_s}}\ (\mathrm{Mpc}/h)^3, \tag{68}$$

[3]Note that the constraints obtained in this way are conservative, because we underestimate the vorticity power spectrum at small scales for large redshift.

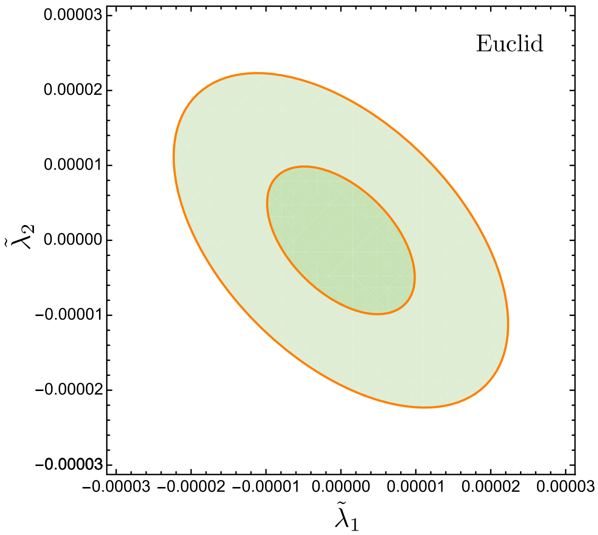

FIG. 1. Constraints on amplitudes of anisotropies for the model (A). We have rescaled the parameters λ_I as $\tilde{\lambda}_I \equiv A_V \lambda_I$. Compare this with the amplitude of the isotropic vorticity power spectrum generated by shell crossing in the standard cold dark matter scenario, where $A_{V,\mathrm{iso}} \sim 10^{-5}$; see, e.g., Ref. [23].

where the power at large scales is given by $n_\ell = 1.3$, the power at small scales is gienv by $n_s = 4.3$, and the transition scale by $k_* = 0.7\ h/\mathrm{Mpc}$. From Fig. 4 of Ref. [23], we find that the predicted amplitude for P_Ω is $A_V = 10^{-5}$.

In Fig. 1, we use this spectrum to estimate the constraints on the eigenvalues $\tilde{\lambda}_{1,2}$. Note that there is no dependence on the fiducial values of the parameters $\tilde{\lambda}_I$ since they enter linearly in the estimator $\hat{\xi}^{2M}_{\ell_1\ell_2}$. Furthermore, the constraints do not depend on the orientation of the eigenvectors due to the block-diagonal structure of the Fisher matrix. The 1σ-constraints on the amplitude of the eigenvalues are $\sigma_\lambda \simeq 6\times 10^{-6}$ with Euclid and even $\sigma_\lambda \simeq 1\times 10^{-7}$ with SKA2. It is also interesting to note that the constraints are better if both eigenvalues have the same sign. This is of course owing to the fact that then the norm of the third eigenvalue is larger. With the SKA and optimistic assumptions, we should therefore be able to constrain an anisotropic vector signal with an amplitude of 1% of the amplitude of the vorticity generated by shell crossing in cold dark matter $A_{V,\mathrm{iso}V} \sim 10^{-5}$ [23].

In Fig. 2, we show the volume of the ellipsoid described by the constraints on (α, β, γ). As we discussed above, the constraint does not depend on the fiducial directions, but it depends on the fiducial values of $\tilde{\lambda}_{1,2}$ or, equivalently, on the choice of A_V and the ratio λ_1/λ_2. In the plot, we fix the *biggest* eigenvalue to $\lambda_{\max} = A_V = 10^{-5}$. The features in the plot can be explained intuitively as follows. We first note that the constraint asymptotes to a constant for $\lambda_1/\lambda_2 > 1$; this is a result of two concurrent effects. On one hand, as we keep the largest eigenvalue, λ_1, fixed, the other, λ_2, becomes smaller, reducing the overall signature of the anisotropy. On the other hand, as the ratio increases, the departure from isotropy is more pronounced, yielding better constraints. Note that we could have fixed the *smallest* eigenvalue equal to A_V; in this case, as the ratio becomes bigger, the overall signature of anisotropy increases, and the two effects add up to give better constraints. Second, the constraints are the worst for $\lambda_1/\lambda_2 = 1$ or $-1/2$. In both cases, this is because we approach a degeneracy: $\lambda_1 = \lambda_2$ or $\lambda_1 = \lambda_3$, respectively. Note that the constraints are slightly better in $\lambda_1 = \lambda_2$ with respect to the second case as the overall amplitude is bigger in this case. The absolute values of the volume show that Euclid constrains the direction of the anisotropy only loosely, while the constraints from SKA2 are excellent, for our choice of amplitude $A_V = 10^{-5}$. Note that the constraint on the volume scales as A_V^3, so that decreasing

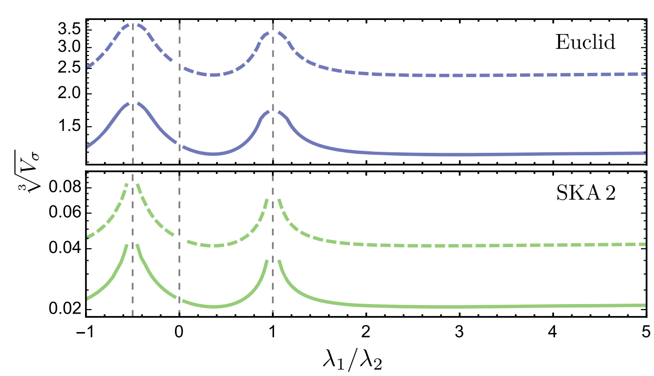

FIG. 2. Volume of the 1σ (solid) and 3σ (dashed) ellipsoids in the $\alpha - \beta - \gamma$ space as a function of the ratio between the λ_A and λ_B. The anisotropic amplitude is set to $A_V = 10^{-5}$. The constraint should be compared to the cube root of the Haar volume $\sqrt[3]{79} \sim 4$.

A_V by an order of magnitude would degrade the bounds in Fig. 2 by a factor 10.

We note here that the galaxy correlation function is of course subject to many systematic effects, arising not least from imperfect modeling of nonlinearities and galaxy bias. However, these sources of theoretical uncertainty would only affect the isotropic part of the signal; it is, e.g., possible for nonlinearities in scalars to leak into vectors. On the other hand, one cannot generate anisotropy from an isotropic configuration. Nonetheless, anisotropy can be a result of the survey geometry or from our Galaxy which blocks a part of the sky and reduces the seeing of the telescope in an anisotropic way. These effects induce an incomplete sky map and may result in anisotropic noise from, e.g., the presence of our Galaxy. Our estimators are chosen to be optimal for a full sky survey and would need to be adjusted appropriately for any other geometry and selection in the standard manner, of course resulting in a reduction of their power. On the other hand, not much credence would be given to the signal if it were found that the anisotropy is closely related to the Galactic plane.

V. CONCLUSIONS

In this paper, we have discussed the effects of an anisotropic vector component in the peculiar velocity field, focusing on the redshift-space distortions induced in the galaxy correlation function. We have presented a general method to isolate the anisotropic signal through a decomposition in bipolar spherical harmonics. We provide an analytical expression for the coefficients of this expansion which does not require the adoption of a specific model. We then show how one can practically use this approach to forecast constraints on the anisotropic sector for two upcoming redshift surveys.

We derive two types of constraints, both on the total amplitude of the anisotropy and on the preferred direction [in terms of the $SO(3)$ volume of its Euler angles]. We can compare our results with the constraints found in Ref. [26] for the isotropic case, which of course has no preferred direction. Given the block-diagonal form of the Fisher matrix, we find that we are able to achieve similar constraints on the amplitude of the vector modes (since we also assume the same shape for the spectrum). Let us, however, note that, even though the constraints are similar, the interpretation of the result in the anisotropic case is cleaner, since in this case the scalar d.o.f. do not contribute to the estimators and therefore they do not need to be accurately modeled.

This work is meant as a study of the feasibility of detecting an anisotropic vector signal in the galaxy two-point function, and together with the analysis carried out in Ref. [26], it represents a comprehensive study of the detectability of vector modes in the correlation function. An interesting future project could be a realistic test of both methods with the help of an artificial survey from N-body simulations. Although measuring the velocity field in N-body simulations is normally challenging [25], this problem is alleviated here as we only need the field at the position of the (observed) galaxies, where it can be directly obtained from the particle velocities. A realistic test would, however, need ray-tracing in the N-body simulation; see, e.g., Refs. [56,57]. To simulate an intrinsic anisotropy, violation of statistical isotropy could be included for example as part of the initial conditions, see, e.g., Ref. [58], or as an external modification of the expansion rate similar in spirit to Ref. [59] (although the authors' concrete example of a Bianchi I model does not contain a vector-type anisotropy) or as an additional vector field, e.g., as in Ref. [60] (where the additional vector d.o.f. would not need to be connected to dark energy; instead we would need a model with non-negligible spatial contributions).

Given a model for the anisotropy, one needs to determine not only the eigenvalues and the directions of its eigenvectors but also the corresponding vector power spectrum. Here, we just assumed this to be given by the vorticity spectrum generated by nonlinear structure formation. This corresponds to a model where an anisotropy only affects the direction but not the strength of the generated vorticity, which is of course not true in general. In full generality, the power spectrum could be reconstructed from the data as a function of multipole and redshift, at the price of much larger error bars.

ACKNOWLEDGMENTS

C. B., R. D., M. K., and V. T. acknowledge funding by the Swiss National Science Foundation. G. C. acknowledges financial support from ERC Grant No. 693024 and Beecroft Trust. I. S. is supported by the European Regional Development Fund and the Czech Ministry of Education, Youth and Sports (Project CoGraDS, No. CZ.02.1.01/0.0/0.0/15_003/0000437).

APPENDIX A: COVARIANCE MATRIX

The variance of the estimator $\xi^{2M}_{\ell\ell'}$ is given by

$$\begin{aligned}\mathrm{var}(\hat{\xi}^{2M}_{\ell\ell'}) &= a_N^2 \sum_{ij}\sum_{km}\langle\Delta_i\Delta_j\Delta_k\Delta_m\rangle X^{2M}_{\ell\ell'}(\hat{x}_{ij},\hat{n}_{ij}) \\ &\quad\times X^{2M*}_{\ell\ell'}(\hat{x}_{km},\hat{n}_{km})\delta_K(x_{ij}-x)\delta_K(x_{km}-x') \\ &= \mathrm{var}_P + \mathrm{var}_M + \mathrm{var}_C. \end{aligned} \tag{A1}$$

Since $\langle\Delta_i\Delta_j\rangle$ contains a Poisson noise contributions and a CV contribution,

$$\langle\Delta_i\Delta_j\rangle = \frac{1}{d\bar{n}}\delta_{ij} + C^{\Delta}_{ij}, \tag{A2}$$

where $d\bar{n}$ is the mean number of galaxies per pixel and the three different contributions to the variance are understood, respectively, as the Poisson term, the mixed term, and the CV term. The first terms is easily found,

$$\begin{aligned}\mathrm{var}_P(x,x') &= \frac{18L_p^{10}}{V^2(xx')^2}\frac{1}{d\bar{n}^2}\sum_{ij}\sum_{km}\delta_{ik}\delta_{jm}X^{2M}_{\ell\ell'}(\hat{x}_{ij},\hat{n}_{ij})\\ &\quad\times X^{2M*}_{\ell\ell'}(\hat{x}_{km},\hat{n}_{km})\delta_K(x_{ij}-x)\delta_K(x_{km}-x')\\ &= \frac{6V}{x^2N^2_{\mathrm{tot}}}\delta_D(x-x'),\end{aligned} \tag{A3}$$

where we have set the factor $(1+(-1)^\ell)=2$ as only even ℓ appear in the expansion. The mixed term is

$$\begin{aligned}\mathrm{var}_M(x,x') &= \frac{18L_p^{10}}{V^2(xx')^2}\frac{1}{d\bar{n}}\sum_{ij}\sum_{km}(\delta_{ik}C^\Delta_{jm}+\delta_{jm}C^\Delta_{ik})\\ &\quad\times X^{2M}_{\ell\ell'}(\hat{x}_{ij},\hat{n}_{ij})X^{2M*}_{\ell\ell'}(\hat{x}_{km},\hat{n}_{km})\\ &\quad\times\delta_K(x_{ij}-x)\delta_K(x_{km}-x')\\ &= \frac{18L_p^{10}}{V^2(xx')^2}\frac{2}{d\bar{n}}\sum_{ij}\sum_{m}C^\Delta_{jm}X^{2M}_{\ell\ell'}(\hat{x}_{ij},\hat{n}_{ij})\\ &\quad\times X^{2M*}_{\ell\ell'}(\hat{x}_{im},\hat{n}_{im})\delta_K(x_{ij}-x)\delta_K(x_{im}-x').\end{aligned}$$

We use the flat-sky expression for C^Δ_{ij},

$$\begin{aligned}C^\Delta_{ij}(\bar{z}) &= \frac{1}{(2\pi)^3}\int d^3k e^{i\mathbf{k}\cdot(\mathbf{x}_j-\mathbf{x}_i)}P(k,\bar{z})(c_0\mathcal{P}_0(\hat{n}\cdot\hat{k})\\ &\quad+c_2\mathcal{P}_2(\hat{n}\cdot\hat{k})+c_4\mathcal{P}_4(\hat{n}\cdot\hat{k})),\end{aligned} \tag{A4}$$

and we perform (in the continuous limit) the following change of variables $\mathbf{y}_j=\mathbf{x}_j-\mathbf{x}_i$, $\mathbf{y}_m=\mathbf{x}_m-\mathbf{x}_i$ together with $\mathbf{x}_i=\mathbf{n}$. We obtain

$$\begin{aligned}\mathrm{var}_M(x,x') &= \frac{24}{\pi N_{\mathrm{tot}}}\int dkk^2P(k,\bar{z})j_\ell(kx)\\ &\quad\times j_\ell(kx')(c_0\beta^0_{\ell\ell'}+c_2\beta^2_{\ell\ell'}+c_4\beta^4_{\ell\ell'}),\end{aligned} \tag{A5}$$

where we have defined the coefficients

$$\begin{aligned}\beta^\sigma_{\ell\ell'} &= (2\ell+1)(2\ell'+1)\begin{pmatrix}\sigma & \ell & \ell\\ 0 & 0 & 0\end{pmatrix}\begin{pmatrix}\sigma & \ell' & \ell'\\ 0 & 0 & 0\end{pmatrix}\\ &\quad\times\begin{Bmatrix}\ell' & \ell & 2\\ \ell & \ell' & \sigma\end{Bmatrix}.\end{aligned} \tag{A6}$$

Finally, the CV term is given by

$$\begin{aligned}\mathrm{var}_C(x,x') &= \frac{18L_p^{10}}{V^2(xx')^2}\sum_{ij}\sum_{km}C^\Delta_{jm}C^\Delta_{ik}X^{2M}_{\ell\ell'}(\hat{x}_{ij},\hat{n}_{ij})\\ &\quad\times X^{2M*}_{\ell\ell'}(\hat{x}_{km},\hat{n}_{km})\delta_K(x_{ij}-x)\delta_K(x_{km}-x'),\end{aligned} \tag{A7}$$

and we can perform a similar change of variable as above $\mathbf{y}_j=\mathbf{x}_j-\mathbf{x}_i$, $\mathbf{y}_m=\mathbf{x}_m-\mathbf{x}_k$ so that, after substituting Eq. (A4) twice, the two exponentials are written as

$$e^{i\mathbf{k}\cdot(\mathbf{x}_m-\mathbf{x}_j)}e^{i\mathbf{k}'\cdot(\mathbf{x}_k-\mathbf{x}_i)}\to e^{i\mathbf{k}\cdot(\mathbf{y}_m-\mathbf{y}_j)}e^{i(\mathbf{k}+\mathbf{k}')\cdot(\mathbf{x}_k-\mathbf{x}_i)}, \tag{A8}$$

and the integral over $\mathbf{x}_k$ enforces $\mathbf{k}=-\mathbf{k}'$. The angular integrals are performed with the properties of BiPoSH as before, and we obtain

$$\mathrm{var}_C(x,x') = \frac{12}{\pi V}\int dkk^2P^2(k,\bar{z})j_\ell(kx)j_\ell(kx')\sum_\sigma\tilde{c}_\sigma\beta^\sigma_{\ell\ell'}, \tag{A9}$$

where

$$\tilde{c}_0 = c_0^2+\frac{c_2^2}{5}+\frac{c_4^2}{9}, \tag{A10}$$

$$\tilde{c}_2 = \frac{2}{7}c_2(7c_0+c_2)+\frac{4}{7}c_2c_4+\frac{100}{693}c_4^2, \tag{A11}$$

$$\tilde{c}_4 = \frac{18}{35}c_2^2+2c_0c_4+\frac{40}{77}c_2c_4+\frac{162}{1001}c_4^2, \tag{A12}$$

$$\tilde{c}_6 = \frac{10}{99}c_4(9c_2+2c_4), \tag{A13}$$

$$\tilde{c}_8 = \frac{490}{1287}c_4^2. \tag{A14}$$

The computation for the off-diagonal covariance matrix, defined in Eq. (58), follows the same steps with the exception that Poisson noise does not contribute for off-diagonal components as it is proportional to $\delta_{\ell_1\ell_2}\delta_{\ell'_1\ell'_2}\delta_{M_1M_2}$. Furthermore, the mixed and cosmic contributions are proportional to $\delta_{M_1M_2}$, and the general case is obtained from Eqs. (A5) and (A9) by substituting the product of spherical Bessel functions inside the integral with $j_{\ell_1}(x)j_{\ell_2}(x')$ and redefining the β coefficients as

$$\begin{aligned}\beta^\sigma_{\ell_1\ell'_1\ell_2\ell'_2} &= i^{\ell_2-\ell_1}\sqrt{(2\ell_1+1)(2\ell'_1+1)(2\ell_2+1)(2\ell'_2+1)}\\ &\quad\times\begin{pmatrix}\sigma & \ell_1 & \ell_2\\ 0 & 0 & 0\end{pmatrix}\begin{pmatrix}\sigma & \ell'_1 & \ell'_2\\ 0 & 0 & 0\end{pmatrix}\begin{Bmatrix}\ell'_1 & \ell_1 & 2\\ \ell_2 & \ell'_2 & \sigma\end{Bmatrix}.\end{aligned} \tag{A15}$$

APPENDIX B: FISHER MATRIX

In this Appendix, we sketch a proof of why the off-diagonal blocks of the Fisher matrix (67) vanish, i.e., $F_{\lambda_A,\alpha_i}=0$. We have

$$F_{\lambda_A,\alpha_i} = \sum_{\{z_{\rm bin}\}}\sum_{i,j}\sum_{\ell_1\ell_1'\ell_2\ell_2'}\sum_M \frac{\partial\xi^M_{\ell_1\ell_1'}(x_i,z)}{\partial\lambda_A} \times \mathrm{cov}^{-1}_{\ell_1\ell_1'\ell_2\ell_2'}(x_i,x_j)\frac{\partial\xi^{M*}_{\ell_2\ell_2'}(x_j,z)}{\partial\alpha_i}$$
$$= \sum_M (Y^*_{2M}(\hat\omega_A) - Y^*_{2M}(\hat\omega_3))\frac{\partial}{\partial\alpha_i}\left(\sum_I \lambda_I Y_{2M}(\hat\omega_I)\right) \times \sum_{\{z_{\rm bin}\}}\sum_{i,j}\sum_{\ell_1\ell_1'\ell_2\ell_2'}\tilde\xi^M_{\ell_1\ell_1'}(x_i,z)\mathrm{cov}^{-1}_{\ell_1\ell_1'\ell_2\ell_2'}(x_i,x_j) \times \tilde\xi^{M*}_{\ell_1\ell_1'}(x_j,z), \quad \text{(B1)}$$

with

$$\frac{\partial}{\partial\alpha_i}\left(\sum_I \lambda_I Y_{2M}(\hat\omega_I)\right) = \sum_I \lambda_I\left(\frac{\partial\theta_I}{\partial\alpha_i}\frac{\partial}{\partial\theta_I} + \frac{\partial\phi_I}{\partial\alpha_i}\frac{\partial}{\partial\phi_I}\right) \times Y_{2M}(\theta_I,\phi_I), \quad \text{(B2)}$$

and (θ_I,ϕ_I) are the polar angles defining the directions of $\hat\omega_I$. We recall that

$$\partial_\theta Y_{2M}(\theta,\phi) = -\frac{\eth+\eth^*)}{2}Y_{2M}(\theta,\phi) = -\frac{\sqrt{6}}{2}({}_1Y_{2M}(\theta,\phi) - {}_{-1}Y_{2M}(\theta,\phi)),$$
$$\partial_\phi Y_{2M}(\theta,\phi) = i\sin\theta\frac{(\eth-\eth^*)}{2}Y_{2M}(\theta,\phi) = i\sin\theta\frac{\sqrt{6}}{2}({}_1Y_{2M}(\theta,\phi) + {}_{-1}Y_{2M}(\theta,\phi)). \quad \text{(B3)}$$

For definiteness, let us consider the case $\lambda_A = \lambda_1$ and $\alpha_i = \alpha$ in Eq. (B1). One has

$$F_{\lambda_1,\alpha} = i\frac{\sqrt{6}}{2}\sum_M (Y^*_{2M}(\hat\omega_1) - Y^*_{2M}(\hat\omega_3)) \times \sum_I \lambda_I \sin\theta_I({}_1Y_{2M}(\hat\omega_I) + {}_{-1}Y_{2M}(\hat\omega_I))[\ldots], \quad \text{(B4)}$$

where the $[\ldots]$ represents the part of the Fisher matrix (B1) which does not depend on $\hat\omega_I$. We recall

$$\sqrt{\frac{4\pi}{2\ell+1}}\sum_{m'} {}_mY_{\ell m'}(\theta_1,\phi_1)\,{}_sY^*_{\ell m'}(\theta_2,\phi_2) = {}_sY^*_{\ell -m}(\beta,\alpha)e^{is\gamma}, \quad \text{(B5)}$$

where here (α,β,γ) are the Euler angles of the rotation rotating the direction (θ_2,ϕ_2) in (θ_1,ϕ_1) and not the angles defined in Eq. (59). In Eq. (B4), the products are between two harmonics evaluated either at the same directions or at orthogonal directions. In our case, we have $\ell = 2$, $s = 0$ and $m = 1$. Furthermore, (β,α,γ) denotes a rotation by either 0 or $\pi/2$ since either $\hat\omega_1 = \hat\omega_2$ or these two vectors enclose an angle of $\pi/2$. In other words, $R(\beta,\alpha,\gamma)\boldsymbol{e}_3 = \pm\boldsymbol{e}_I$ where $I\in\{1,2,3\}$ and $Y_{\ell m}(\beta,\alpha) = Y_{\ell m}(R^{-1}(\beta,\alpha,\gamma)\boldsymbol{e}_3) = Y_{\ell m}(\pm\boldsymbol{e}_I)$; see Ref. [61]. The Euler angle γ is irrelevant here since a rotation around $\boldsymbol{e}_z$ leaves $\boldsymbol{e}_z$ invariant. But for the Cartesian axes $\boldsymbol{e}_I$, ϑ is either 0 or $\pi/2$, and $Y_{21}(\vartheta,\varphi)\propto \sin\vartheta\cos\vartheta$ vanishes. This completes the proof that the off-diagonal boxes in the Fisher matrix vanish.

APPENDIX C: $\xi^{2M}_{\ell\ell'}$

The explicit expressions for the real-space version of Eqs. (43)–(45) are given by

$$\xi^{2M(\mathrm{a})}_{\ell\ell'} = -\frac{16\pi^{3/2}}{45}C^\Omega_\ell(z,x)\sum_I \lambda_I Y^*_{2M}(\hat\omega_I) \times \left(\delta_{\ell,0}\delta_{\ell',2} + 2\sqrt{\frac{2\ell'+1}{5}}\begin{pmatrix}2 & 2 & \ell'\\ 0 & 0 & 0\end{pmatrix}\delta_{\ell,2}\right), \quad \text{(C1)}$$

$$\xi^{2M(\mathrm{b})}_{\ell\ell'} = -\frac{16\pi^{3/2}}{5}C^\Omega_\ell(z,x)\sqrt{(2\ell+1)(2\ell'+1)} \times \sqrt{\frac{2}{15}}\sum_I \lambda_I Y^*_{2M}(\hat\omega_I) \times \left[2\begin{pmatrix}3 & 1 & \ell\\ 0 & 0 & 0\end{pmatrix}\begin{pmatrix}3 & 1 & \ell'\\ 0 & 0 & 0\end{pmatrix}\begin{Bmatrix}1 & 2 & 1\\ \ell & 0 & \ell'\end{Bmatrix} + 3\begin{pmatrix}1 & 1 & \ell\\ 0 & 0 & 0\end{pmatrix}\begin{pmatrix}1 & 1 & \ell'\\ 0 & 0 & 0\end{pmatrix}\begin{Bmatrix}1 & 2 & 1\\ \ell & 1 & \ell'\end{Bmatrix}\right], \quad \text{(C2)}$$

$$\xi^{2M(\mathrm{c})}_{\ell\ell'} = -\frac{16\pi^{3/2}}{15}C^\Omega_\ell(z,x)\sum_I \lambda_I Y^*_{2M}(\hat\omega_I) \times \left[\frac{1}{5}\delta_{\ell,2}\delta_{\ell',0} + \frac{8}{105}\sqrt{2\ell+1}\begin{pmatrix}4 & 2 & \ell\\ 0 & 0 & 0\end{pmatrix}\delta_{\ell',4} + \frac{4}{7\sqrt{5}}\sqrt{2\ell+1}\begin{pmatrix}2 & 2 & \ell\\ 0 & 0 & 0\end{pmatrix}\delta_{\ell',2}\right]. \quad \text{(C3)}$$

[1] R. Durrer, M. Kunz, and A. Melchiorri, Cosmic structure formation with topological defects, Phys. Rep. **364**, 1 (2002).

[2] D. Daverio, M. Hindmarsh, M. Kunz, J. Lizarraga, and J. Urrestilla, Energy-momentum correlations for Abelian Higgs cosmic strings, Phys. Rev. D **93**, 085014 (2016); Erratum, Phys. Rev. D **95**, 049903(E) (2017).

[3] J. Lizarraga, J. Urrestilla, D. Daverio, M. Hindmarsh, and M. Kunz, New CMB constraints for Abelian Higgs cosmic strings, J. Cosmol. Astropart. Phys. 10 (2016) 042.

[4] R. Durrer, T. Kahniashvili, and A. Yates, Microwave background anisotropies from Alfven waves, Phys. Rev. D **58**, 123004 (1998).

[5] L. H. Ford, Inflation driven by a vector field, Phys. Rev. D **40**, 967 (1989).

[6] A. Golovnev, V. Mukhanov, and V. Vanchurin, Vector inflation, J. Cosmol. Astropart. Phys. 06 (2008) 009.

[7] T. Jacobson and D. Mattingly, Gravity with a dynamical preferred frame, Phys. Rev. D **64**, 024028 (2001).

[8] T. G. Zlosnik, P. G. Ferreira, and G. D. Starkman, Modifying gravity with the Aether: An alternative to dark matter, Phys. Rev. D **75**, 044017 (2007).

[9] L. Heisenberg, Generalization of the Proca Action, J. Cosmol. Astropart. Phys. 05 (**2014**) 015.

[10] G. Tasinato, Cosmic acceleration from Abelian symmetry breaking, J. High Energy Phys. 04 (2014) 067.

[11] E. A. Lim, Can we see Lorentz-violating vector fields in the CMB?, Phys. Rev. D **71**, 063504 (2005).

[12] M. Nakashima and T. Kobayashi, The music of the Aetherwave–B-mode polarization in Einstein-Aether theory, Phys. Rev. D **84**, 084051 (2011).

[13] D. Saadeh, S. M. Feeney, A. Pontzen, H. V. Peiris, and J. D. McEwen, A framework for testing isotropy with the cosmic microwave background, Mon. Not. R. Astron. Soc. **462**, 1802 (2016).

[14] L. Ackerman, S. M. Carroll, and M. B. Wise, Imprints of a primordial preferred direction on the microwave background, Phys. Rev. D **75**, 083502 (2007); Erratum, Phys. Rev. D **80**, 069901(E) (2009).

[15] N. Bartolo, A. Kehagias, M. Liguori, A. Riotto, M. Shiraishi, and V. Tansella, Detecting higher spin fields through statistical anisotropy in the CMB and galaxy power spectra, Phys. Rev. D **97**, 023503 (2018).

[16] P. A. R. Ade *et al.* (Planck Collaboration), Planck 2015 results. XVI. Isotropy and statistics of the CMB, Astron. Astrophys. **594**, A16 (2016).

[17] A. R. Pullen and C. M. Hirata, Non-detection of a statistically anisotropic power spectrum in large-scale structure, J. Cosmol. Astropart. Phys. 05 (2010) 027.

[18] D. Jeong and M. Kamionkowski, Clustering Fossils from the Early Universe, Phys. Rev. Lett. **108**, 251301 (2012).

[19] M. Shiraishi, N. S. Sugiyama, and T. Okumura, Polypolar spherical harmonic decomposition of galaxy correlators in redshift space: Toward testing cosmic rotational symmetry, Phys. Rev. D **95**, 063508 (2017).

[20] N. S. Sugiyama, M. Shiraishi, and T. Okumura, Limits on statistical anisotropy from BOSS DR12 galaxies using bipolar spherical harmonics, Mon. Not. R. Astron. Soc. **473**, 2737 (2018).

[21] J. Adamek, D. Daverio, R. Durrer, and M. Kunz, General relativity and cosmic structure formation, Nat. Phys. **12**, 346 (2016).

[22] J. Adamek, D. Daverio, R. Durrer, and M. Kunz, Gevolution: A cosmological N-body code based on general relativity, J. Cosmol. Astropart. Phys. 07 (2016) 053.

[23] S. Pueblas and R. Scoccimarro, Generation of vorticity and velocity dispersion by orbit crossing, Phys. Rev. D **80**, 043504 (2009).

[24] G. Jelic-Cizmek, F. Lepori, J. Adamek, and R. Durrer, The generation of vorticity in cosmological N-body simulations, J. Cosmol. Astropart. Phys. 09 (2018) 006.

[25] O. Hahn, R. E. Angulo, and T. Abel, The properties of cosmic velocity fields, Mon. Not. R. Astron. Soc. **454**, 3920 (2015).

[26] C. Bonvin, R. Durrer, N. Khosravi, M. Kunz, and I. Sawicki, Redshift-space distortions from vector perturbations, J. Cosmol. Astropart. Phys. 02 (**2018**) 028.

[27] R. Durrer, *The Cosmic Microwave Background* (Cambridge University Press, Cambridge, England, 2008).

[28] T. H.-C. Lu, K. Ananda, C. Clarkson, and R. Maartens, The cosmological background of vector modes, J. Cosmol. Astropart. Phys. 02 (2009) 023.

[29] G. Cusin, V. Tansella, and R. Durrer, Vorticity generation in the Universe: A perturbative approach, Phys. Rev. D **95**, 063527 (2017).

[30] N. Kaiser, Clustering in real space and in redshift space, Mon. Not. R. Astron. Soc. **227**, 1 (1987).

[31] D. Jeong and F. Schmidt, Large-scale structure observables in general relativity, Classical Quantum Gravity **32**, 044001 (2015).

[32] R. Durrer and V. Tansella, Vector perturbations of galaxy number counts, J. Cosmol. Astropart. Phys. 07 (2016) 037.

[33] J. Yoo, A. L. Fitzpatrick, and M. Zaldarriaga, A new perspective on Galaxy clustering as a cosmological probe: General relativistic effects, Phys. Rev. D **80**, 083514 (2009).

[34] C. Bonvin and R. Durrer, What galaxy surveys really measure, Phys. Rev. D **84**, 063505 (2011).

[35] A. Challinor and A. Lewis, The linear power spectrum of observed source number counts, Phys. Rev. D **84**, 043516 (2011).

[36] T. Baldauf, U. Seljak, L. Senatore, and M. Zaldarriaga, Galaxy bias and non-linear structure formation in general relativity, J. Cosmol. Astropart. Phys. 10 (2011) 031.

[37] D. Jeong, F. Schmidt, and C. M. Hirata, Large-scale clustering of galaxies in general relativity, Phys. Rev. D **85**, 023504 (2012).

[38] V. Tansella, C. Bonvin, R. Durrer, B. Ghosh, and E. Sellentin, The full-sky relativistic correlation function and power spectrum of galaxy number counts. Part I: Theoretical aspects, J. Cosmol. Astropart. Phys. 03 (2018) 019.

[39] D. Varshalovich, A. Moskalev, and V. Khersonskiĭ, *Quantum Theory of Angular Momentum: Irreducible Tensors, Spherical Harmonics, Vector Coupling Coefficients, 3nj Symbols* (World Scientific, Singapore, 1988).

[40] A. Hajian and T. Souradeep, Measuring statistical isotropy of the CMB anisotropy, Astrophys. J. **597**, L5 (2003).

[41] A. Hajian and T. Souradeep, The Cosmic microwave background bipolar power spectrum: Basic formalism and applications, arXiv:astro-ph/0501001.

[42] S. Basak, A. Hajian, and T. Souradeep, Statistical isotropy of cmb polarization maps, Phys. Rev. D **74**, 021301 (2006).
[43] A. R. Pullen and M. Kamionkowski, Cosmic microwave background statistics for a direction-dependent primordial power spectrum, Phys. Rev. D **76**, 103529 (2007).
[44] G. Cusin, C. Pitrou, and J.-P. Uzan, Are we living near the center of a local void?, J. Cosmol. Astropart. Phys. 03 (2017) 038.
[45] L. G. Book, M. Kamionkowski, and T. Souradeep, Odd-parity bipolar spherical harmonics, Phys. Rev. D **85**, 023010 (2012).
[46] A. F. Heavens and A. N. Taylor, A spherical harmonic analysis of redshift space, Mon. Not. R. Astron. Soc. **275**, 483 (1995).
[47] A. J. S. Hamilton and M. Culhane, Spherical redshift distortions, Mon. Not. R. Astron. Soc. **278**, 73 (1996).
[48] A. S. Szalay, T. Matsubara, and S. D. Landy, Redshift space distortions of the correlation function in wide angle galaxy surveys, Astrophys. J. **498**, L1 (1998).
[49] I. Szapudi, Wide angle redshift distortions revisited, Astrophys. J. **614**, 51 (2004).
[50] P. Papai and I. Szapudi, Non-perturbative effects of geometry in wide-angle redshift distortions, Mon. Not. R. Astron. Soc. **389**, 292 (2008).
[51] D. Bertacca, R. Maartens, A. Raccanelli, and C. Clarkson, Beyond the plane-parallel and Newtonian approach: Wide-angle redshift distortions and convergence in general relativity, J. Cosmol. Astropart. Phys. 10 (2012) 025.
[52] G. Arfken and H. Weber, *Mathematical Methods for Physicists* (Harcourt Academic, New York, 1966).
[53] A. Messiah, *Quantum Mechanics*, 12th ed. (North Holland Publishing Co., Amsterdam, 1981), Vol. 2.
[54] R. Laureijs *et al.*, Euclid definition study report, arXiv:1110.3193.
[55] E. Villa, E. Di Dio, and F. Lepori, Lensing convergence in galaxy clustering in ΛCDM and beyond, J. Cosmol. Astropart. Phys. 04 (2018) 033.
[56] A. Barreira, C. Llinares, S. Bose, and B. Li, RAY-RAMSES: A code for ray tracing on the fly in N-body simulations, J. Cosmol. Astropart. Phys. 05 (**2016**) 001.
[57] M.-A. Breton, Y. Rasera, A. Taruya, O. Lacombe, and S. Saga, Imprints of relativistic effects on the asymmetry of the halo cross-correlation function: From linear to non-linear scales, arXiv:1803.04294.
[58] C. Pitrou, T. S. Pereira, and J.-P. Uzan, Weak-lensing by the large scale structure in a spatially anisotropic universe: Theory and predictions, Phys. Rev. D **92**, 023501 (2015).
[59] A. S. Schmidt, S. D. M. White, F. Schmidt, and J. Stucker, Cosmological N-body simulations with a large-scale tidal field, Mon. Not. R. Astron. Soc. **479**, 162 (2018).
[60] E. Carlesi, A. Knebe, G. Yepes, S. Gottloeber, J. Beltran Jimenez, and A. L. Maroto, N-body simulations with a cosmic vector for dark energy, Mon. Not. R. Astron. Soc. **424**, 699 (2012).
[61] R. Durrer, *The Cosmic Microwave Background* (Cambridge University Press, Cambridge, England, 2008).